Separation of alkenes with organic and inorganic composite membranes

Kruger, A, Krieg, H and Neomagus, H
North West University, Chemistry, North West University, Chemical Engineering

Keywords: Ceramic composite membranes, NaA zeolite, Teflon AF2400, Alkene separation

Abstract-In this study the separation of two alkenes, ethene and butene, which have similar physical properties, was attempted for industrial gas purification. Using both inorganic (ceramic and zeolite NaA) and polymeric (Teflon AF 2400) coated ceramic membranes, a mixture of 70 % ethene and 30 % butene was separated. Both membranes showed promising single gas permeation, where the best inorganic ideal selectivity ($\alpha = 9$), was obtained for the NaA coated ceramic membrane. The Teflon AF 2400 coated ceramic membrane had an ideal selectivity of 31. For the binary mixture, the NaA coated ceramic membrane was however not able to separate the mixture satisfactorily, probably due to intercrystalline boundary diffusion. The Teflon coated membrane yielded a selectivity o 4 with a permeate permeance of 1.98×10^{-3} $mol.s^{-1}.m^{-2}.bar^{-1}$.

INTRODUCTION

Steam cracking of naphtha (mixture of flammable hydrocarbons) is commonly used for the production C4's olefins of which ethylene and butene form part of the products (Bakker et al., 1997). Olefins such as ethene and butene are widely used in synthetic applications. One of ethene's many uses is as an ethylene propylene combination for making rubber (Free patents, 2009). Butene also fills an important role in the rubber industries, as it can produce a form of polyethylene by co-polymerisation of ethylene and butene that is more flexible and more resilient than other resins (Static Shell, 2009). Furthermore, ethylene and butene can be converted to the more valuable propene via metathesis (Liu et al., 2010)**.**

Currently, cryogenic distillation is commonly used for the separation of alkenes and it is well known that this separation technique is highly energy (and thus cost) intensive (Kaufmann et al., 1994)**.** In an attempt to find environmentally friendly and cheaper separation techniques, olefin and paraffin's separations have been investigated with various types of membranes (Mulder, 1996). Polymer membranes like Matrimid, Pyralin 2566 and Torlon AI-10 were used to investigate the separation of propylene/propane mixtures (Merkel et al., 2000). Traditional composite membranes like MFI, grown on an α-alumina support, were tested for n-C_4H_{10}/n-/i-C_4H_{10} separation, where an ideal selectivity of 15 was obtained (Yuko et al., 2002). Polymer-inorganic nano composite membranes, PTMSP-silica (poly(trimethylsilylpropyne)), and nano composite membranes were also tested for C_4H_{10}/CH_4 separation.

Although the separation of ethene and butene are of industrial importance, a membrane process has not been evaluated for this separation. It is well known that zeolite based separations are predominantly dependent on molecular size differences, since their selectivity is largely based on a sieving effect. On the other hand, separations in polymeric membranes are dependent on the solubility and diffusion of the gasses. With the small difference in molecular size of ethene and butene, the permeation of these olefins through a polymeric membrane could be largely attributed to differences in solubility, which is a function of the critical temperature (Lin and Freeman, 2004). However, in spite of a critical temperature difference of 144.1 °C (Freeman and Pinnau, 1999 & Merkel et al., 2000), a kinetic diameter difference of 0.6 A (Encyclopaedia, 2008) and a difference in mole weight (g/mol) of 28, which relates to molecular size, the separation of ethene and butene remains an industrial challenge.

To investigate the membrane facilitated separation of ethene and butene, two composite membranes were investigated. In both instances a ceramic support was used. However, the thin selective film consisted of either a NaA zeolitelayer or a polymeric Teflon AF 2400 layer (Fig.1).

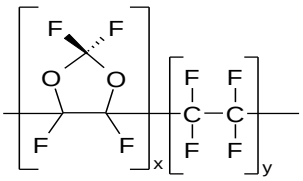

Figure 1 : Teflon AF 2400, where y = x – 1 [6]

Both these proposed coatings have advantages and disadvantages. One possible disadvantage of the polymer coated composite membrane is its thermal stability which however is not a significant problem since Teflon AF2400 has a glass transition temperature of 240 °C. On the other hand, it is well known that zeolite membranes especially Al rich zeolites, like NaA, have the disadvantage of intercrystalline boundaries being formed between close-packed crystals (Pinnau and Toy, 1996). It is the purpose of this study to evaluate the suitability of the two in-house manufactured composite membranes for the separation of ethene and butene.

EXPERIMENTAL

Synthesis

Synthesis of ceramic support

A tubular α-alumina support (21 mm outer diameter, 18 mm inner diameter, 1.5 mm in thickness and 5.5 cm in length) was manufactured in-house by centrifugal casting as discussed previously (Bisset, 2005). For this study, AKP15 powder (Sumitomo Chemical Company, Ltd., Japan) was used. The sintering temperature was 1200 °C. After washing the sintered support and ensuring the correct length of the support, the support was irradiated with UV-light (HOK 4/120 [400W]) in deionized water for 12 hours on each side to improve zeolite adhesion (Zah et al., 2007). The support was then sonified for 3 x 5 min with deionized water and dried overnight in a conventional hot-air oven at 120 °C. Before zeolite synthesis, the exterior of the support was wrapped in PTFE tape to ensure that the zeolite would only grow on the inside of the support.

Synthesis of NaA coated membrane

The first layer for the NaA was synthesized from two reactant mixtures with the first solution having a weight ratio of 10.1 % sodium metasilicate pentahydrate ($Na_2SiO_3 \cdot 5H_2O$), 76.6 % deionized H_2O and 13.3 % NaOH (NaOH pellets; Merck, analytical grade, in deionised water). The second solution was prepared with a 1.8 % anhydrous aluminate ($NaAlO_2$:41 % Na2O, 54 % Al_2O; Riedel- Haen/Fluka), 79.2 % deionized H2O and 19 % NaOH by weight. These two solutions were aged, while stirred, separately for 1 h at room temperature before adding the aluminate to the silicate solution. This final solution which had the following molar oxide composition 48.9 Na_2O:1 Al_2O3:5.08 SiO_2:979.2 H_2O was aged for 30 min while stirring at room temperature. The ceramic support was then soaked with 15 mL of this solution in a Teflon-lined autoclave for 30 min at room temperature, while rotating in the oven. Subsequently, the zeolite synthesis was done at 85 °C for 4 h using a conventional hot-air oven. After 4 h, the oven was switched off and left to cool for 3 h while rotating. After the first synthesis the membrane was sonified in an ultrasonic bath (Integral systems) with deionised water (6 x 10 min; second synthesis only 3×10 min) to clear extra solution and to neutralize the membrane. The second layer was synthesized exactly the same as the first layer, the only difference was that no saturation (30 min soaking period) was necessary.

Synthesis of Teflon coated membrane

A solution was made from Teflon AF 2400 (DuPont 3M) by dissolving it in FC-77 (3M) with a weight percentage of 5 %. After taping the α-ceramic support with PTFE on the outside, it was dip coated in the Teflon solution twice and left to dry overnight in a desicator at room temperature. After drying, the membrane was heated to 170^{o}C for 2 hours, to facilitate the adhesion to the support.

Morphology and crystallinity

Mercury Porosimetry

Mercury porosimetry (Micrometritics Autopore IV, mercury porosimeter) was used to determine the average pore size and porosity of the support.

SEM

Dry samples of the membranes were coated with Au/Pd (80/20) in vacuum. SEM images were taken with a FEI Quanta 200 ESEM instrument. This technique was used to evaluate the surface roughness of the ceramic support as well as the appearance of the coated layers. SEM images were used to study the surface morphology by ensuring a closed formed zeolite on the support with no visible defects, and to obtain the zeolite layer thickness. For the Teflon AF2400, SEM images were used to establish the presence of tears in the Teflon layer and to estimate the Teflon thickness.

XRD

The XRD (Rontgen system, Cu tube at 40 kV and 45 mA) data was used to confirm the Si/Al ratio and the morphological structure of the NaA membrane and to determine that the crystal structure is representative of NaA.

Single gas permeation

The experimental setup for the single gas permeation is shown in Figure. 2. The dead end module (**3**), which contained the membrane, was placed in a conventional oven (**1**) and the temperature was controlled by a relay-connected thermocouple. The pressure was monitored with an absolute pressure gauge (**4** ASHCROFT), while the permeate (**2**) flow was measured with a downstream soap-film meter (**5**) which was open to the atmosphere.

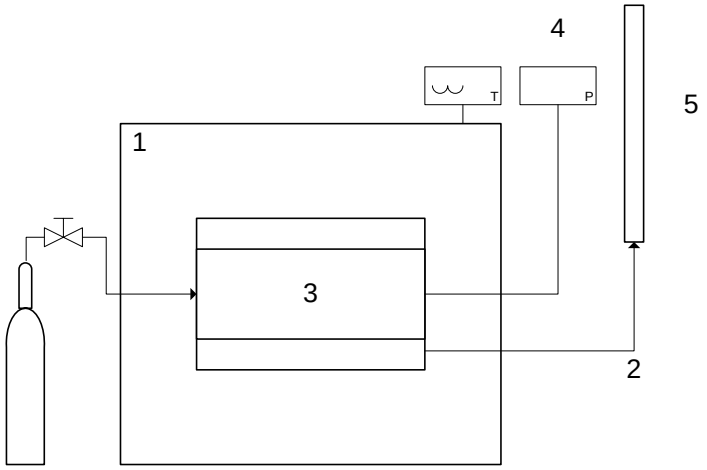

Figure 2 : Experimental setup for single gas permeation

By measuring the flow rate ($mL.min^{-1}$) and converting it to molar flux ($mol.m^{-2}.s^{-1}$), the permeance ($mol.m^{-2}.s^{-1}.bar^{-1}$) can be obtained as the slope of the molar flux vs pressure differential graph. The average thickness of the coated membrane layers, which was obtained from the cross-section of the SEM micrographs (example shown in Figure 7(b)) was 5 µm for the NaA coated layer, 5 µm for the Teflon coated layer and 1.5 mm for the ceramic support. The ideal selectivities that are presented where obtained from the molar fluxes of the individual gases.

Support

The ceramic support on its own could not be characterized with He, N_2 and SF_6 due to the very high permeabilities observed. The permeance of both ethene and butene was measured at pressures ranging from 0.2 – 0.5 bar between 50 – 150 °C.

NaA

The NaA membrane was characterized with He, N_2 and SF_6. The ethene and butene permeation studies were done in the pressure differential range of 0.2 – 1 bar between 50 – 150 °C.

Teflon AF2400

The Teflon coated membrane was characterized with He, N_2 and CO_2. Ethene and butene permeation was measured at 0.2 – 1 bar between 50 – 150 °C.

Binary permeation

A diagram of the experimental setup for the binary permeation is given in Figure. 3. The flow rate of the feed mixture (**1**) was controlled by mass flow controllers (**7**), which were individually calibrated. A 70/30 (ethene/butene) volume percentage mixture, based on a current process stream ratio, was used as the feed phase for separation. A conventional oven (**2**) was used with a relay-thermal couple, to regulate the temperature. An absolute pressure gauge (**5** ASHCROFT) and backpressure gauges (**3** Delta Trans) ensured correct trans-membrane pressures. Both permeate and retentate permeation was measured using separate bubble flow meters (**4**). A gas chromatograph (**6**, Carbo Erba, GC 6000 VEGA SERIES) was used to measure the quantity of each component in the permeate and retentate. The pipelines from the reactor to the GC were purged with the carrier gas, He, to ensure accurate measurements.

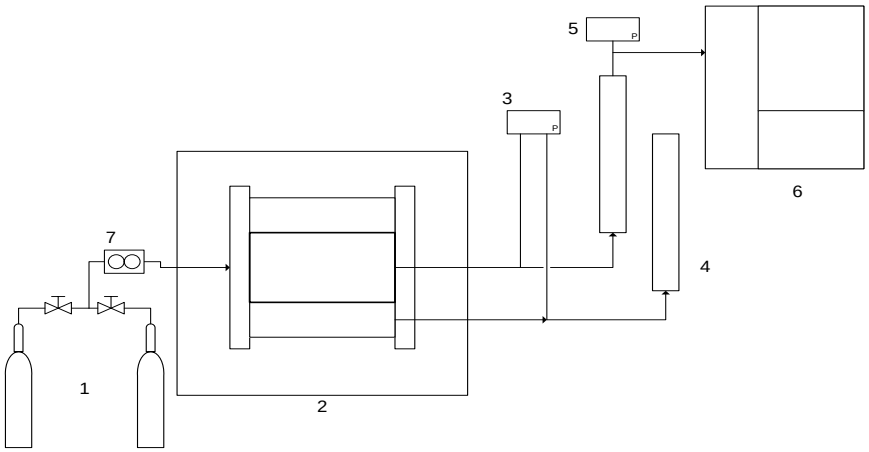

Figure 3 : Experimental setup for binary gas permeation

The total flow for the feed was set to 50 mL.min-1 and all the binary permeation experiments were done at 1 bar (inlet) and ambient pressure (permeate pressure) with the 70/30 (ethene/butene) mixture, while the temperature was varied over the 0 – 150 °C range. For calibration of the mass flow controllers, the fraction of ethene/butene in the feed was varied and GC analysis was used to obtain a calibration curve of peak area vs fraction in feed, without passing through the membrane. The mole concentration was converted to volume concentration. The separation factor (selectivity for the mixture permeation) was obtained by calculating the separation factor using

$$\alpha = \frac{\frac{X_a}{X_b}}{\frac{Y_a}{Y_b}}$$

x_a and x_b is the volume concentration of the feed (in this case 70/30) and y_a and y_b the volume concentration of the permeate. The selectivity was calculated using the average of multiple readings for both membranes.

RESULTS AND DISCUSSION

Morphology and crystallinity

Mercury porosimetry measurements indicated that the ceramic support structure had an average pore size of 167 nm and a porosity of 37 %.

Support

When using centrifugal casting, larger particles are deposited on the outside (outer layer), while the smaller particles are deposited on the inside (inner layer) surface. Figure 4.a shows the outer layer (top-view) of the ceramic support where the larger particles accumulated and Figure 4.b the smaller particles on the inner layer (cross section). This implies that the inside surface of the ceramic tube is smooth, facilitating a good bonding strength for the coating to the support as well as a thin defect free coating layer.

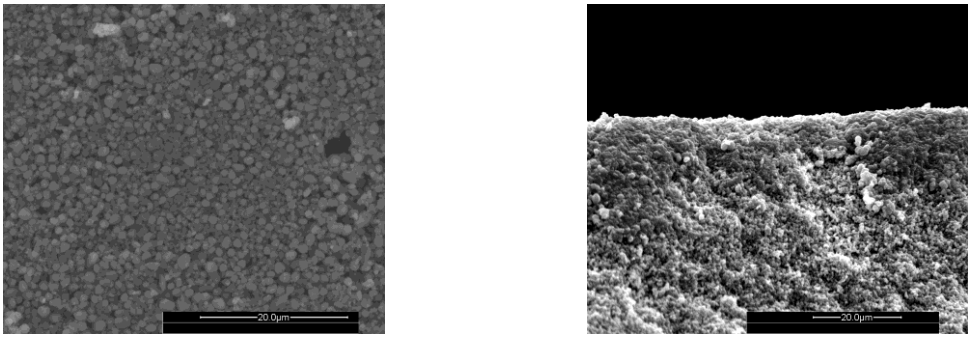

(a) (b)

Figure 4 : SEM images of (a) top-view of the outer and (b) cross-section of the inner layer view of the ceramic support

NaA membrane

Figure 5.a depicts a closed packed NaA membrane formation with no imperfections or any visible voids present. According to Figure 5.b the average thickness of the NaA membrane was approximately 5 µm, coated on the inside of the ceramic support.

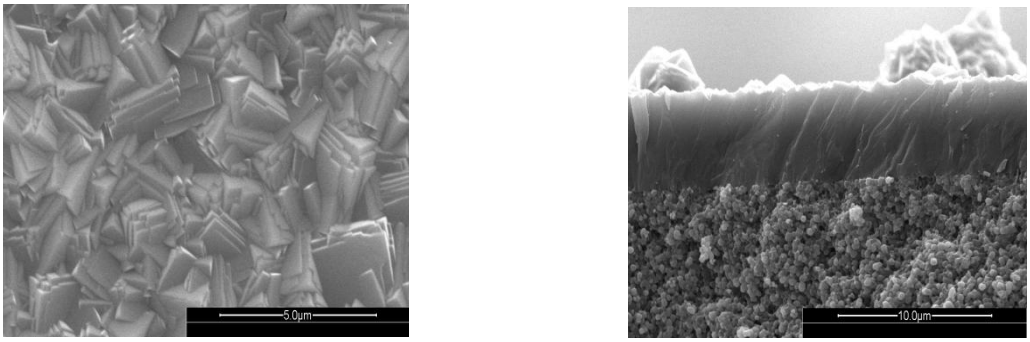

(a) (b)

Figure 5 : SEM images of (a) top-view and (b) side view for the NaA coated ceramic support

XRD (Fig. 6) analysis confirmed that the ratio of the Si/Al is representative of a NaA membrane. The peak fingerprint confirmed that this was indeed a NaA-1 sample (Izasc, 2009).

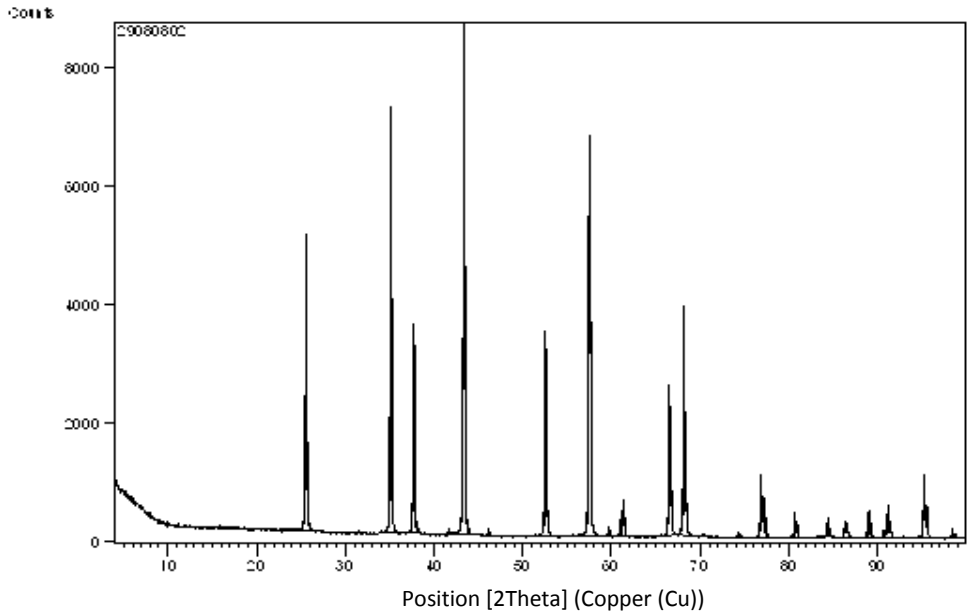

Figure 6 : XRD of a NaA membrane

Teflon coated membrane

SEM images (Fig. 7.a) for the Teflon coated membrane showed a closed layer of Teflon on top of the support with no visible tears or cracks. The Teflon thickness was approximately 5 μm.

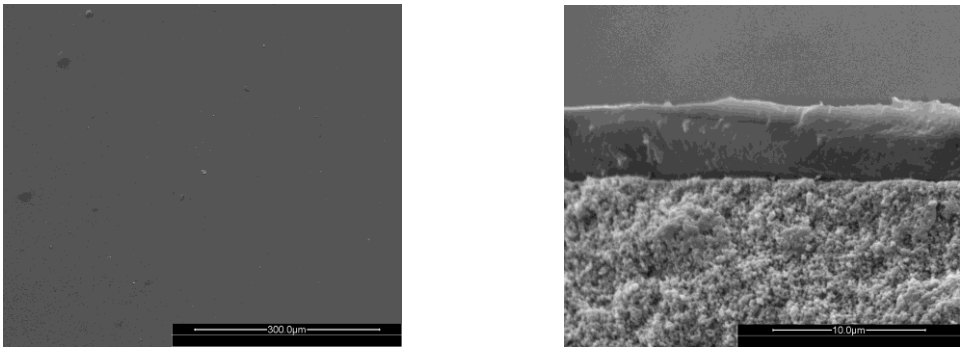

(a) (b)

Figure 7 : SEM images of (a) top-view and (b) side view of a Teflon AF 2400 coated ceramic membrane

Single gas permeation

Support

The single gas permeation and ideal selectivity of both ethene and butene is shown in Figure 8 and Figure 9 respectively. The low pressure differentials mentioned in Section 2.3.1 were used because of the high permeability of the ceramic support. The permeances presented in Figure 8 and 9 are the average values obtained from various repetitions over the 0.2 – 0.5 bar pressure differential range tested for each temperature. It is clear from Figure 8 that the permeance of ethene is unaffected by temperature in the temperature range 50^{o}C – 150 °C, while butene seems to show a decrease in permeance with increasing temperature.

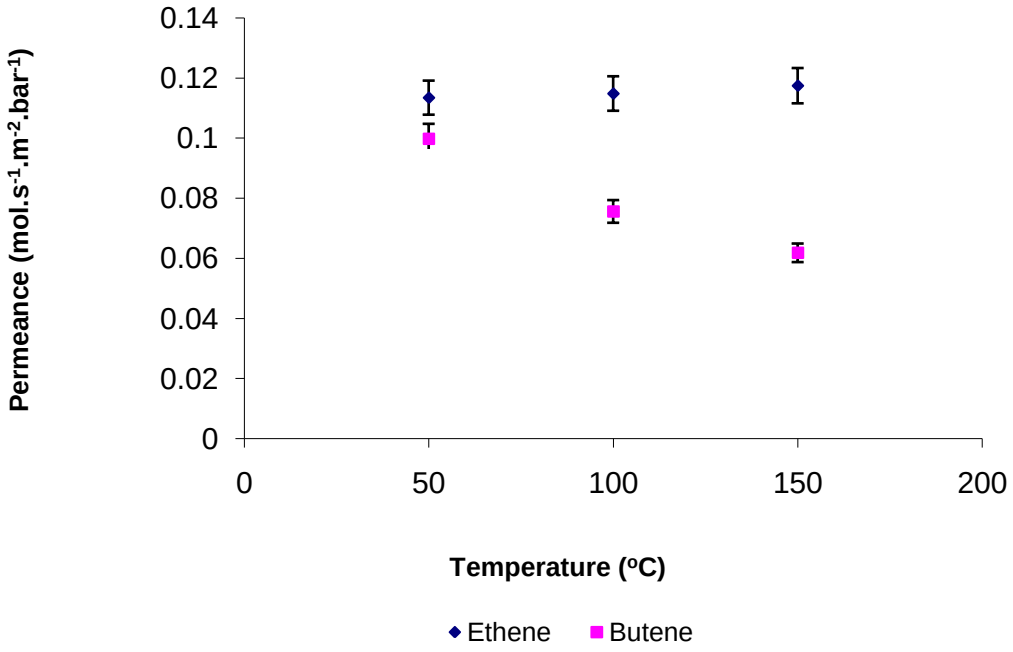

Figure 8 : Permeance of ethene/butene through the ceramic support

The overall mass transport of pure non-absorbable gas through porous materials could be considered as the sum of both Knudsen and Poiseuille flux. However, when considering that the pore sizes of the ceramic support are in the 150 – 200 μm (See Section 3.1) it is assumed that the majority of flux is due to Knudsen flow.

The pore size is in the 160 μm range & thus it can be assured that Poiseuille flux is dominant. In addition low pressure differentials were used for the support and according to

$$\lambda = \frac{kT}{\pi d^2 \sqrt{2}}$$

the pressure is inversely proportional to the mean free path (λ) which is indicative to Knudsen flow (Mulder, 1996). Furthermore it was stated in Section 3.3.1 that butene has a larger kinetic diameter which according to the equation has a quadratic effect on λ thereby increasing the Poiseuille contribution to the butene flux. Thereby increasing the temperature, and thus λ will increase, implies that the butene has a larger Poiseuille component at lower temperature than ethene therefore as the temperature is increased the Knudsen component of the flux for butene increases more than the Knudsen contribution of flux for ethene with increasing temperature. This explains why the butene permeance decreased with increased temperature as ethene had Knudsen flow at low temperature the permeance remained the same with increasing temperature.

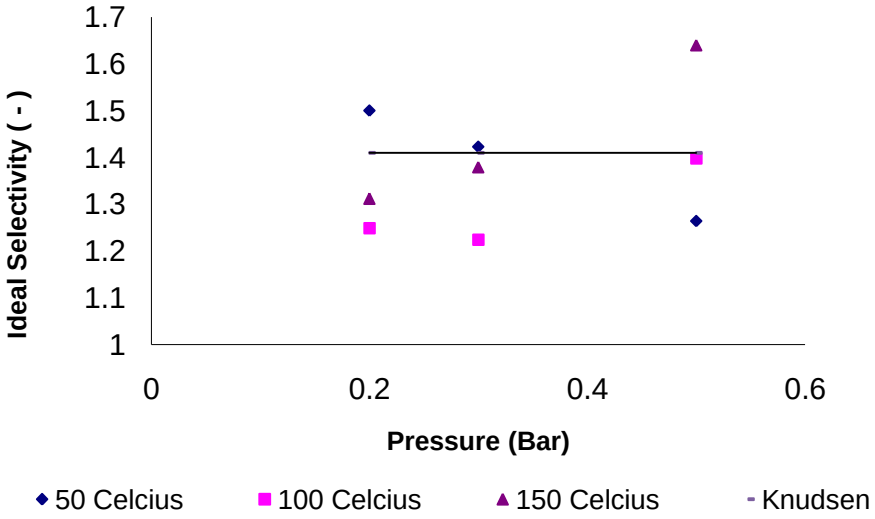

Figure 9 : Ideal selectivity of ethene/butene for ceramic support. The line represents the calculated Knudsen selectivity for ethene/butene

According to Figure 8 the selectivity will favor ethene at higher temperatures while the permeances of both gasses are comparable at 50 °C. This effect implies, as can be seen in Figure 9, that low temperatures will benefit Knudsen flow more, due to the low pressures used, than Poiseuille flow. The selectivity will however increase when higher pressures are used and the Knudsen component is reduced in the total flux. From Figure 8 and 9, the best permeance obtained was 0.117 $mol.s^{-1}.m^{-2}.bar^{-1}$ (150 °C) for ethene and 0.0891 $mol.s^{-1}.m^{-2}.bar^{-1}$ (50°C) for butene while the best ideal selectivity(1.64) was obtained at 150 °C and 0.5 bar trans membrane pressure.

NaA membrane

The single gas permeance (Fig.10) for both ethene and butene remained constant initially (50 °C and 100 °C), but decreased at 150 ^{o}C. This decreasing permeance of ethene and butene with increasing temperature can partly be related to the temperature dependence on the molecular kinetic diameter of a molecule. Molyneux showed that the permeation activation energy increases with increasing molecular diameter (Molyneux, 2008). Therefore, an increased temperature can lead to increased molecular bonding vibrations of both gasses, which can temporarily increase the molecular kinetic diameter. This fluctuating size increases can be related to the decrease in the permeation rate to an average of 0.00186 $mols^{-1}m^{-2}bar^{-1}$ for ethene and 0.000191 $mol.s^{-1}m^{-2}bar^{-1}$ for butene at 150 °C.

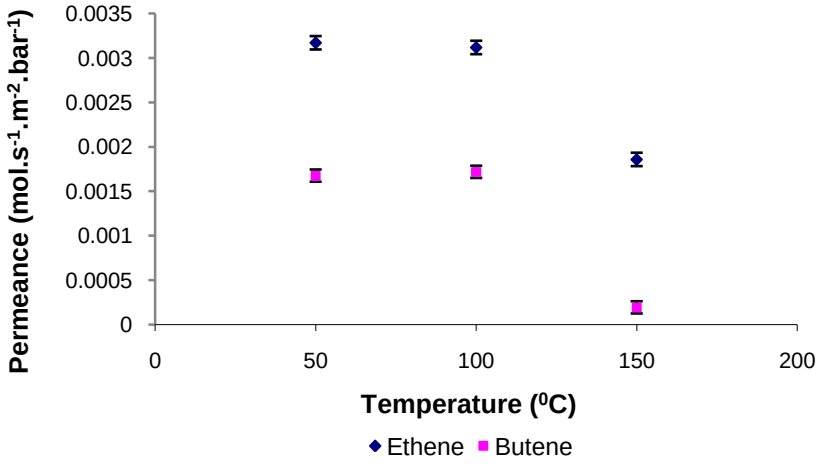

Figure 10 : Permeance of ethene/butene for NaA membrane

The size fluctuation mentioned above is more prominent for butene than ethene. With butene having a kinetic diameter of 4.5 A (Xu etal., 2000), any increase in size would decrease butene permeance through the NaA zeolite which has an average pore size of 4.1 A (Zah etal., 2007). No permeation would be expected on size difference alone, but

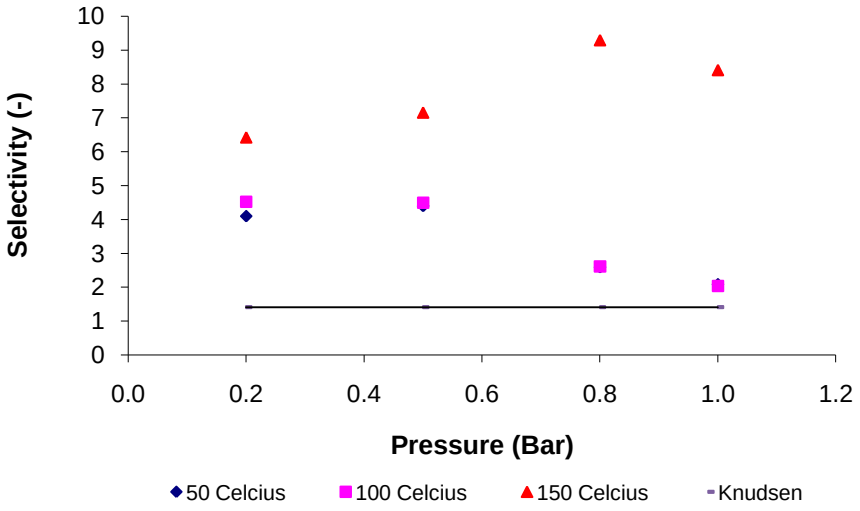

Figure 11 : Ideal selectivity of ethene/butene for NaA membrane

However, irrespective of the pressure differential or temperature, the NaA coated ceramic membrane yielded selectivities above Knudsen. This, in combination with the nearly 100 fold decrease in permeance with and without the NaA coating confirms the absence of defects or pinholes in the NaA coating.

Teflon coated membrane

For the single gas permeation studies through the Teflon coated ceramic membrane, the permeation of the separate gasses showed no significant variation of permeance with increasing temperature (Fig 12) with anaverage butene permeation 0.00022 mol.$s^{-1}m^{-2}bar^{-1}$, which was aproximately 16 times slower than the average ethene permeation of 0.00347 mol.s^{-1}.m2.bar^{-1}.

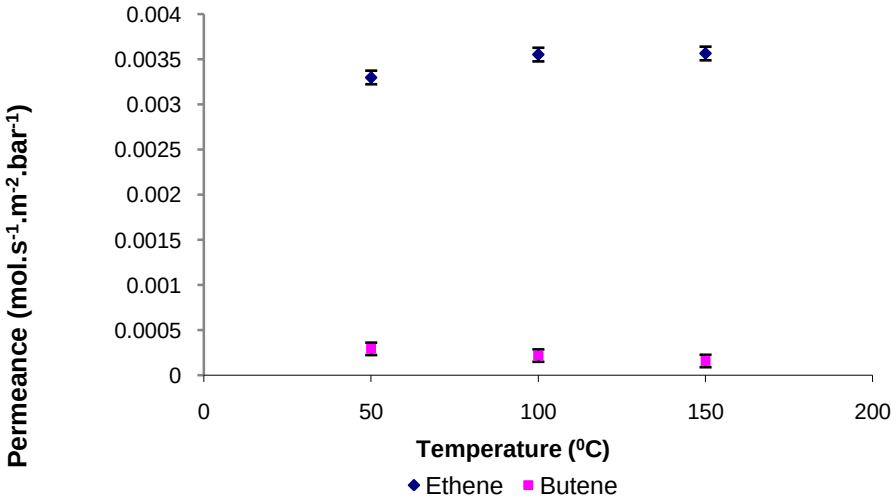

Figure 12 : Permeance of ethene/butene for Teflon AF 2400

The low variation in permeability at different temperatures for both gasses fits well with the fact that the gas permeability of Teflon AF 2400 has previously been shown to have low temperature dependence when tested for methane, ethane and propane permeance (Pinnau and Toy, 1996). While the ethene permeation through the Teflon layer was higher than that of butene, it was also near identical to the ethene permeation observed for the NaA layer at 50 and 100 ^{o}C (see Fig. 10). The permeance of the butene however decreased significantly in comparison to the NaA layer membrane.

In Fig. 13 the ideal selectivities of ethene and butene through the Teflon coated membrane is presented. The selectivity's for the lower pressures, not shown in Fig. 13 could not be calculated due to the low permeation rate of butene.

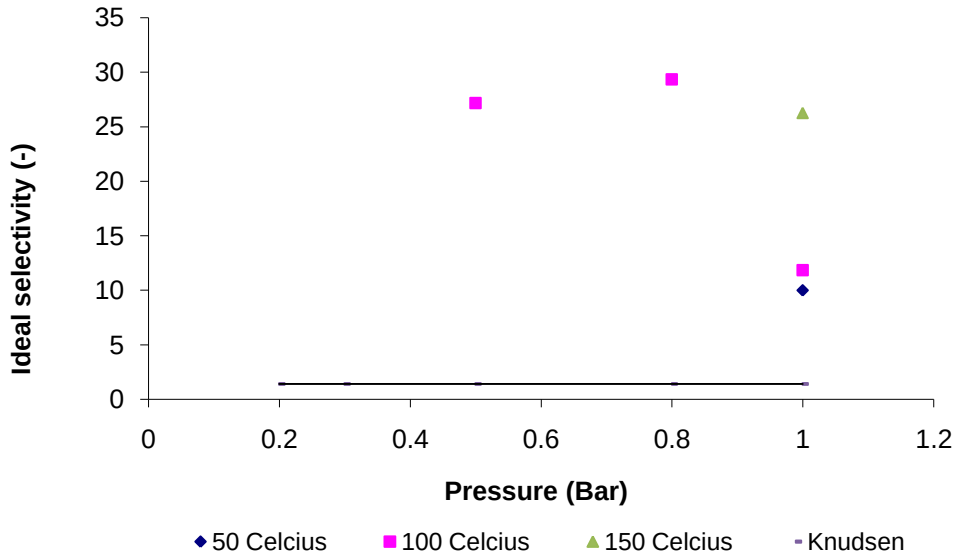

Figure 13 : Ideal selectivity of ethene/butene for Teflon coated membrane

When comparing the two coated membranes (NaA and Teflon AF2400) with each other it is clear that ethene permeates faster than butene irrespective of the investigated variables. Gas permeation through the NaA membrane is primarily based on size and diffusion, while through the Teflon membrane it is based firstly on solubility and then diffusion as Teflon is a non-porous polymer. The lowest ideal selectivity (highest selectivity of 29.3) for the Teflon AF2400 is 11 where the NaA could only reach 10. Thus according to the single gas permeation, ethene should permeate much faster through the Teflon coated membrane than butene. The NaA coated membrane should also allow ethene to permeate faster than butene at 150 ^{o}C, however with lower selectivities than the Teflon coated membrane.

Mixture permeation

The calibration curve shown in Figure. 14 was obtained for the GC analyses showing the correlation between the peak areas (of the individual gasses) and the volume fraction for the range of 0 – 100 %, in the permeate. All experiments were done at the 70/30 ethene/butene (vol/vol) fraction, 1 bar pressure differential and the three temperatures. The choice of the 70/30 ratio was based on the actual industrial requirement.

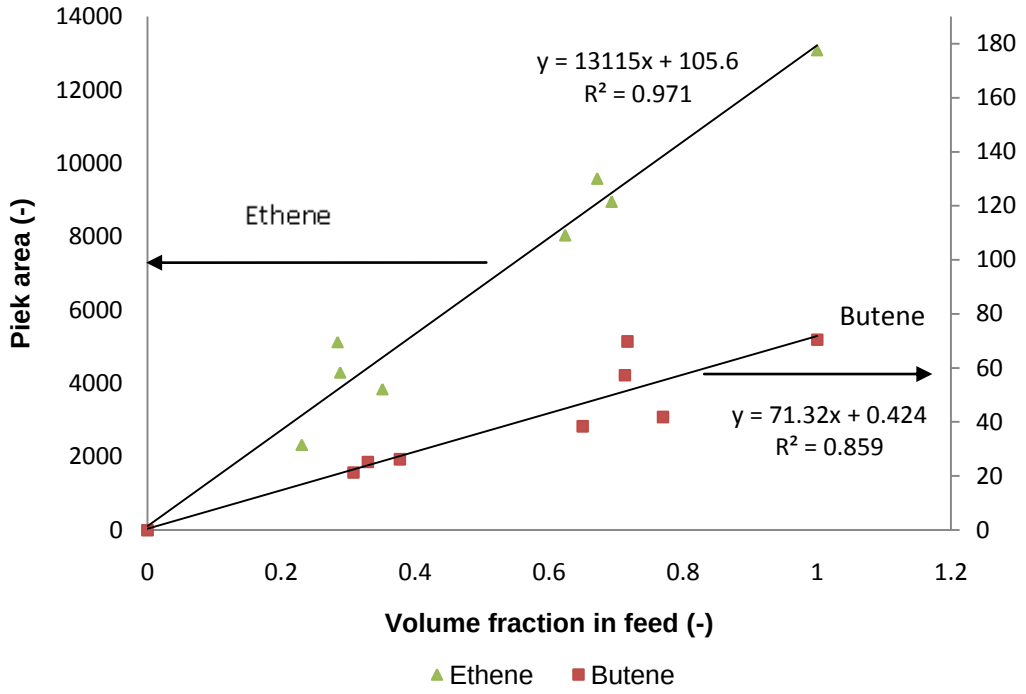

Figure 14 : Calibration curve of the GC analyses for binary mixtures

In Table 1, the permeance and selectivity data obtained at 3 different temperatures and 1 bar is presented for the NaA separation, while Table 2 shows the same for the Teflon coated membrane. The percentage error refers to the deviation of each reading from the average permeance (0.00052 $mol.s^{-1}m^{-2}bar^{-1}$ for the NaA and 0.00198 $mol.s^{-1}m^{-2}bar^{-1}$ for the Teflon AF 2400 membrane) of all readings. The actual selectivity for the NaA coated membrane shows a small increase with increasing temperature as has been observed with the ideal selectivity obtained for the single gas permeation (Fig. 11). It should be noted that the selectivity for the NaA studies were calculated by dividing the ethene with the butene permeance. However for the Teflon AF2400 studies the butene permeance was divided with the ethene permeance to obtain an answer of unity. The selectivity for the Teflon AF 2400 coated membrane also showed an increase with increasing temperature between 50 – 100 ^{o}C, but at 150 ^{o}C the selectivity decreased significantly.

Table 1 : NaA permeance and selectivity for the 70/30 ethene/butene mixture at 1 bar

Temperature ^{o} (C)	Separation factor (-)	Best ideal Selectivity (Section 3.2)	Permeance ($mol.s^{-1}.m^{-2}.bar^{-1}$)	% Error on separation factor
50	1.22	4.4	$4.40x10^{-04}$	19
100	1.27	4.5	$7.52x10^{-04}$	19
150	1.42	9.3	$3.69x10^{-04}$	24

Table 2 : Teflon AF2400 permeance and selectivity for the 70/30 ethene/butene mixture at 1 bar. Note that the separation factor favors butene.

Temperature ^{o} (C)	Separation factor (-)	Best ideal Selectivity (Section 3.2)	Permeance ($mol.s^{-1}.m^{-2}.bar^{-1}$)	% Error on separation factor
50	1.22	10	$2.08x10^{-03}$	-
100	1.27	29	$1.98x10^{-03}$	16
150	1.42	27	$1.89x10^{-03}$	-

What is significant however is the fact that for the NaA coated membrane the ideal and actual selectivity was in both cases in favor of the ethene. However, for the Teflon coated membrane the actual selectivity was in favor of the butene although ethene had the higher permeance during the single gas studies. It will be shown in the following section that the parameters that influence the gas permeation in non-porous membranes, such as Teflon AF2400, are both determined by the membrane properties as well as the gas interactions with the membrane.

NaA membrane

It is clear from Table 1 that the actual selectivity is lower than the ideal selectivity obtained by the single gas permeation. A higher selectivity would be expected for the separation when looking only at the kinetic diameters of ethene and butene (3.9 A and 4.5 A) (Molyneux, 2008 & Xu etal., 2000) and the NaA zeolite pore sizes (4.1 A), which suggests that the NaA should be ideally suited to facilitate this separation. This was however not observed. The reason is probably, as previously reported, that there are intercrystalline boundaries between Al containing zeolite cell units, which give a lower resistant path for the gas molecules to permeate through the membrane (Zah etal., 2007). Since the Knudsen flow is determined by the molecular weight, it can be expected that smaller gas molecules (ethene) will have higher fluxes than larger molecules (butene) resulting in ideal selectivities which are higher than actual selectivity, where competition will hinder the transport of the smaller molecule. This was observed with a drop in selectivity from 9 (ideal selectivity, Section 3.2.2) to 1.4 (actual selectivity, Section 3.3). The Knudsen selectivity for ethene/butene is 1.41, which correlates with the separation factor observed for the NaA membrane confirming that the flow through the membrane was probably due to Knudsen flow.

Teflon coated membrane

According to the peak areas relating to the selective permeation, it is clear that the butene permeated (0.0677 mols-1m-2bar-1) faster than the ethene in the binary study relative to the maximum peak areas according to the calibration curves. This was not the opposite tendency when compared to the single gas permeance of ethene and butene where the ethene permeance was higher than that of butene irrespective of the temperature and the pressure differential. However, the binary result can possibly be explained in terms of the solubility and diffusivity properties of the gasses in the mixture. It is well known that composite membrane permeation through polymers is based on the solubility and diffusivity of the gasses as expressed in P = DS, with P the permeability ($mol.s^{-1}.m^{-2}.bar^{-1}$), D the diffusivity ($cm^3.s^{-1}$) and S the solubility ($cm^3cm^{-3}cmHg^{-1}$) of the gas. While solubility is a function of the gas condensability, gas interaction with the polymer and the free volume of the polymer, diffusivity is a function of the molecule size, which is also related to the free volume of the polymer and chain flexibility of the polymer. For, for any gas to permeate through a polymeric non-porous membrane, it must first dissolve (solubility) into the membrane before it can diffuse (diffusivity) through the polymeric membrane. The general rule is that the solubility coefficient (S) will increase as the critical temperature increases (Lin and Freeman, 2004). This means that butene (Tc = 155 °C) will be more soluble than ethene (Tc = 9.5 °C) because it is more condensable. This was also the findings of Shon *et al.* who reported that the permeability coefficients were not only affected by molecular size but by critical temperatures (Shon et al., 2000). It can thus be concluded that butene was more soluble in the Teflon than ethene. Since one can accept that smaller molecules usually have a higher mobility (and hence diffusivity) through a polymer, it is clear that for the interaction between the Teflon and the ethene/butene mixture, the solubility was more important for the binary mixture than the diffusion rate. By hindering the ethene from dissolving in the polymer, the effective concentration of the ethene in the polymer decreased resulting in a higher overall permeability of the butene. With the Knudsen selectivity at 1.41, the Teflon coated membrane clearly yielded a superior selectivity with the best separation factor of 3.97 which was obtained at 100 ^oC and 1 bar. The separation factors obtained in this study are comparable to values obtained by Pinnau & Toy (Pinnau and Toy, 1996), who found mixed gas separation factors between 0.8 and 5 for various gas mixtures including a CH_4/N_2 selectivity of 0.8 and a CO_2/N_2 selectivity of 5. Although the conditions differ from this study it shows that the range of selectivity's is comparable.

CONCLUSION

In this study we demonstrated the manufacture of both NaA zeolite and a Teflon AF 2400 coated ceramic membranes. The ideal selectivities obtained for the NaA membrane varied between 2 and 10 in favor of ethene. However, the membrane showed low actual selectivity and is probably not suitable for ethene/butene separation due to the intercrystalline boundaries, which determine the path that the molecules follow. Subsequently, it can be concluded that the transport for this membrane was diffusion (pressure) driven rather than solubility driven.

The ideal selectivities obtained for the Teflon AF 2400 were higher (between 11 and 30 in favor of ethene) than the values obtained for the NaA membrane . However, when evaluating the performance using an actual ethene and butene mixture (70/30, vol/vol), the separation factor varied between 1.22 to 3.97 in favor of butene. This reversal of preference can be attributed to the difference in transport obtained for the dense polymer material, where the permeance is a function of the solubility and diffusivity. It seems that during competitive transport the higher solubility of butene dominates the possible improved diffusivity of the ethene. It was thus shown that both ethene or butene could be preferentially permeated through the membrane based on the choice of the active membrane layer.

REFERENCES

1. W.J.W Bakker, L.J.P. van den Broeke, F. Kapteijn, J.A. Moulijn, Temperature dependence of one-component permeation through a silicalite-1 membrane, Am. Inst. Chem. Eng., 43 (1997) 2203.
2. H. Bisset, Manufacture and Optimization of tubular ceramic membrane supports, M.Sc Dessertation, North-West University, 2005, p35, 36.
3. http://encyclopedia.airliquide.com/encyclopedia.asp?gasid=11 [20/10/08]
4. http://encyclopedia.airliquide.com/encyclopedia.asp?LanguageID=11&CountryID=19&Formula=C2H4&GasID=0&UNNumber=&btnFormula.x=0&btnFormula.y=0 [20/10/08]
5. B. D. Freeman and I. Pinnau, "Polymeric Materials for Gas Separations". in B. D. Freeman and I. Pinnau (Eds.), Polymer Membranes for Gas Vapor Separation, ACS Symp. Ser., 733 (1999) 2.
6. http://www.freepatentsonline.com/4288358.html [13/01/09]
7. http://izasc.ethz.ch/fmi/xsl/IZA-SC/mat_xrd.xsl?-db=crystal_data&-lay=web&-recid=87&-find= (31/05/2009).
8. E. A. Kaufman, J. A. Moss, J. L. Jnr. Pickering, Cryogenic Distallation. Patent 5372009, December 13, 1994.
9. H. Lin, B.D. Freeman, Gas solubility, diffusivity and permeability in poly(ethylene oxide), J. Membrane Sci., 239 (2004) 105-117.
10. S. Liu, X. Li, W. Xin, S. Xie, P. Zeng, L. Zhang, L. Xu, Cross metathesis of butane-2 and thene to propene over Mo/MCM-22-Al2O3 catalysts with different Al2O3 contents, J. Nat. Gas Chem. 19 (2010) 482-486.
11. T. C. Merkel, V. I. Bondar, K. Nagai, B. D. Freeman, and I. Pinnau, Gas Sorption, Diffusion, and Permeation in Poly(dimethylsiloxane), J. Polymer Sci., Part B: Polym. Phys., 38 (2000) 415-34.
12. P. Molyneux, Permeation of gases through microporous silica hollow-fiber membranes: Application of the transition-site model, J. Membrane Sci., 320 (2008) 42-56.
13. M. Mulder, Basic Principles of Membrane Technology, 2nd ed, Kluwer Academic Publishers, p. 227, ISBN : 0 – 7923 – 4248 – 8.
14. M. Mulder, Basic Principles of Membrane Technology, 2nd ed, Kluwer Academic Publishers, p.7, ISBN 0 – 7923 – 4248 – 8.
15. Pinnau, L.G. Toy, Gas and vapour transport properties of amorphous perfluorinated copolymer membranes based on 2,2-bistrifluoromethyl-4,5-difluoro-1,3- dioxole/tetrafluoroethylene, J. Membrane Sci., 109 (1996) 125-133.
16. M.T. Ravanchi, T. Kaghazchi, A Kargari, Application of membrane separation processes in petrochemical industry: a review, Desalination. 235 (2009) 199-244.
17. W. Shon, D. Ryu, S.Oh, J. Koo, A study on the development of composite membranes for the separation of organic vapors, J. Membrane Sci. 175 (2000) 163-170.
18. http://www.static.shell.com/static/chemicals/downloads/responsible_energy/butene_product_stewardship_summary.pdf [13/01/09]
19. J. Towfighi, H. Zimmermann, R. Karimzadeh, M. M. Akbarnejad, Steam Cracking of Naphta in Packed Bed Reactors, Ind. Eng. Chem. Res. 41 (2002) 1419-1424.
20. O.Ullaland, Fluid systems for RICH detectors, Nucl. Instr. Meth. Phys. Res. A553 (2005) 107–113.
21. X. Xu, W. Yang, J. Liu and L. Lin, Fast formation of NaA zeolite membrane in the microwave field, Sci. Press. 45 (2000).
22. Y. Yampolskii, I. Pinnau and B.D. Freeman, Materials Science of Membranes for Gas and Vapor Separation, Wiley-Interscience, New York (2006).
23. T. Yuko, T. Tsuru, T. Yoshioka, M. Asaeda, Gas permeation properties of MFI zeolite membranes prepared by the secondary growth of colloidal silicalite and application to the methylation of toluene. J. Membrane Sci., 54 (2002) 257-268.
24. J. Zah, H.M. Krieg , J.C. Breytenbach , Single gas permeation through compositionally different zeolite NaA membranes: Observations on the intercrystalline porosity in an unconventional, semicrystalline layer, J. Membrane Sci., 287 (2007) 300–310.